African Journal of Agricultural Research Vol. 5(20), pp. 2817-2824, 18 October, 2010
Available online at http://www.academicjournals.org/AJAR
ISSN 1991-637X ©2010 Academic Journals

Full Length Research Paper

An operational approach for estimating surface vapor pressure with satellite-derived parameter

Yaohuan Huang, Dong Jiang* and Dafang Zhuang

Data Center for Resources and Environmental Sciences, State Key Lab of Resources and Environmental Information System, Institute of Geographical Sciences and Natural Resources Research, Chinese Academy of Sciences, China.

Accepted 27 September, 2010

Surface vapor pressure (SVP) is a highly significant variable for physically based crop growth simulating and crop yield modeling. Regional spatially representative data of observed SVP are not currently available. However, an excellent correlation has been found between SVP and precipitable water vapor (PWV) with many previous works. Based on the correlation analysis between satellite-derived PWV data moderate resolution imaging spectroradiometer (MODIS) atmospheric profile product dataset and daily mean SVP data calculated from 37 ground-based meteorology stations measurements in Haihe River Basin of North China, an operational scheme for estimating daily SVP with satellite-derived PWV data was proposed in this study. The accuracy of the approach was evaluated through comparisons with *in situ* measurements. The explained variance is 0.838 with a root-mean-squared-error (RMSE) of 2.912 hPa. The results indicated that the proposed method is an effective way to obtain SVP data at a regional scale.

Key words: Haihe river basin, surface vapor pressure, precipitable water vapor.

INTRODUCTION

Surface vapor pressure (SVP) is a partial atmospheric pressure that attributes to water vapor in the air as one of the most important climatic variables adopted in agricultural system models to simulate fluxes and states of water and carbon (Waring et al., 1998). Therefore deriving information on spatial-temporal distribution of SVP is essential in understanding the crop growth and water availability. However, regional spatially representtative data of observed SVP are not currently available. SVP data is conventionally calculated with several primary data including air temperature, humility and vapor density, which is measured in a relative sparse network of ground-based meteorological stations. Quite a few spatial interpolation algorithms have been widely used to convert point data to a continuous raster surface, including thin plate splines (Hutchinson et al., 1994), Thiessen polygons (Thiessen, 1911), Ordinary Kriging (Brooker, 1979), Inverse-Distance weighting (Watson et al., 1985), Truncated Gaussian Filtering (Thornton et al., 1997). These spatial interpolation techniques may not be suitable for the measurement stations are often too sparse for implementing an interpolation scheme in most regions (New et al., 1999).

Precipitable water vapor (PWV) is described as the total amount of water vapor in the zenith direction between the underlying surface and the top of the atmosphere. The correlation between PWV and SVP has been established for a long term (Karalis et al., 1974). Monteith found a linear relationship between the logarithm of PWV and the square root of vapor pressure when 30 characteristic air masses were correlated with British Isles crossed (Monteith, 1961). Idso found that the correlation coefficient between the logarithm of PWV and the square root of vapor pressure at Phoenix, Ariz. was 0.913, which was derived from 190 *in situ* measurements during three summers (Idso, 1969). Reber established a liner model between PWV and SVP when studying the correlation of PWV and surface absolute humidity at the stations of San Nicolas Island, Point Mugu and China Lake, California in 1970 (Reber et al., 1972). Yang derived an empirical expression to calculate the PWV based on the ground and radiosonde data at 20 stations in China from 1992 to 1993, which indicated that the PWV was well related to SVP (Yang et al., 1996). Li analyzed the relationship between PWV and SVP in North China and established

*Corresponding author. E-mail: jiangd@igsnrr.ac.cn. Tel: +86-10-64889433. Fax: +86-10-64855049.

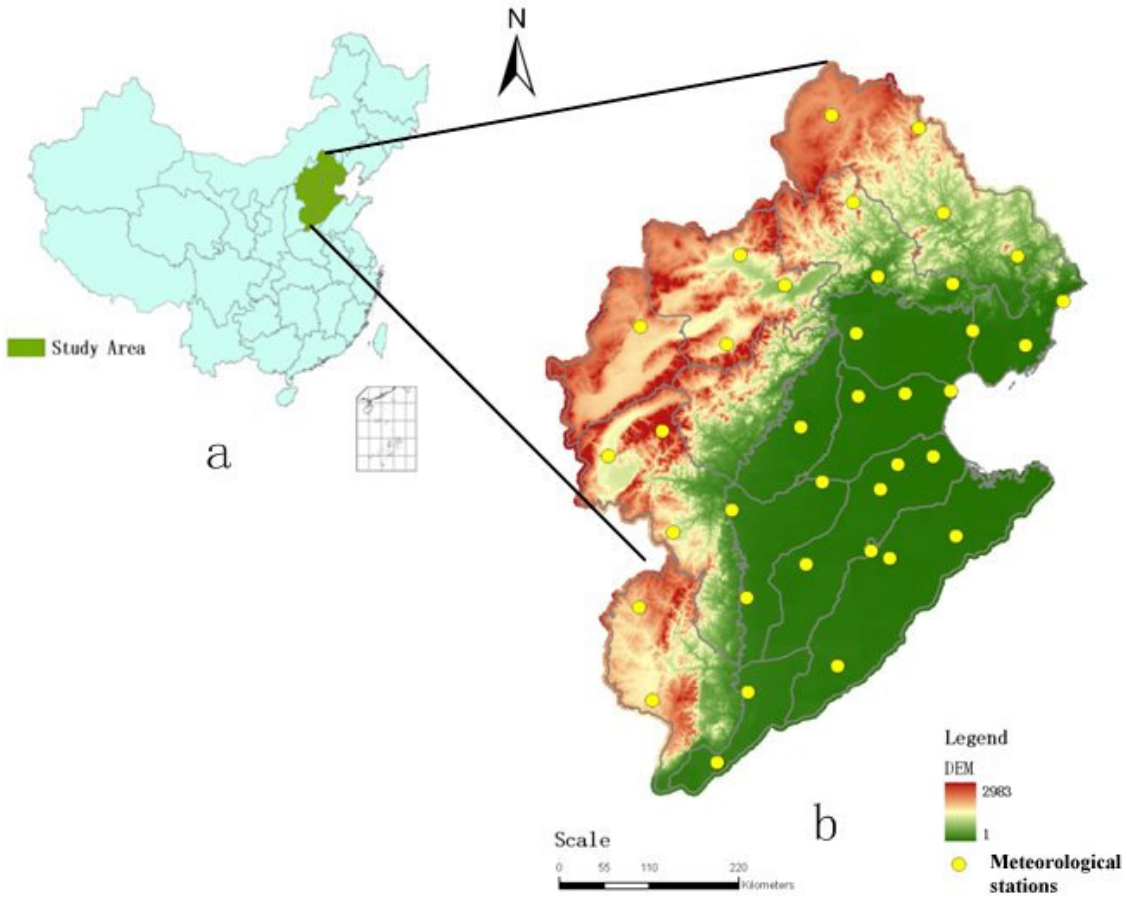

Figure 1. Location of the study region: Haihe River Basin, North China.

empirical formulas with a linear regression method (Li et al., 2009). Similar researches have been continued to the present, indicating that PWV is a variable strongly related to SVP.

With the development of the remote sensing technique, PWV has become a common subject in detection (Prince et al., 1998; Green et al., 2002; Kern et al., 2008). Various algorithms have been proposed to retrieve the PWV from satellite data with a variety of electromagnetic spectrums or instruments including global positional system (GPS), infrared, near infrared and microwave (Barton et al., 1999; Bevis et al., 1994; Chylek et al., 2003; Duan et al., 1996; Ottle et al., 1999a, b; Westwater et al., 2001). PWV data retrieved from remote sensing data are better spatial and temporal data sources than conventional *in-situ* observations. First, satellite observations can provide global coverage of PWV potentially in various time intervals. Second, fewer calculations are required in a simple transfer function such as from a regression than in an interpolation scheme (Hashimoto et al., 2008; Hong et al., 2008). For example, daily atmospheric profile product datasets are presented routinely from NASA EOS data Gateway (EDG) based on the moderate resolution imaging spectroradiometer (MODIS) observations.

The objective of this study is to invest the correlation between satellite-derived PWV data and SVP data calculated from *in-situ* stations in Haihe River Basin of North China. Then, a straightforward scheme was established for obtaining SVP data operationally. The results of the method were evaluated with data of 37 ground-based meteorological stations in the study region, Haihe River Basin.

Study region

As the study area, Haihe River Basin in North China is located from 34°09′N to 43°11′N ,111°21′E to 120°43′E , as illustrated in Figure 1. The Haihe River basin covers Beijing, Tianjin, the most part of Hebei, a part of Shandong, Henan, Shanxi and Inner Mongolia with an area of 318,000 km^2, of which mountains and plateaus cover 189,000 km^2, accounting for 60%, while plains cover 129,000 km^2, accounting for 40%. The region is dominated by semi-humid continental monsoon climate with its multi-year average annual precipitation of 535 mm. The locations of 37 meteorological stations in this area are also shown in Figure 1.

Table 1. Positions and widths of five MODIS near-IR channels used in water vapor retrievals.

MODIS Channel	Position (μm)	With (μm)	Resolution (m)
2	0.865	0.040	250
5	1.240	0.020	250
17	0.905	0.030	1000
18	0.936	0.010	1000
19	0.940	0.050	1000

MATERIALS AND METHODS

Data acquisition

Satellite-derived PWV data

Satellite-derived PWV data were downloaded from the MODIS atmospheric profile product dataset from NASA EDG (http://modis.gsfc.nasa.gov/index.php). The PWV data is daily produced at 5 × 5 km pixel resolution. The MODIS atmospheric water-vapor (precipitable water vapor) product is an estimation of the total tropospheric column water vapor obtained from integrated MODIS infrared retrievals of atmospheric moisture profiles in clear scenes (http://modis-atmos.gsfc.nasa.gov/MOD07_L2/index.html). Five near-IR channels of MODIS instrument are described as useful for retrieving PWV. The details of them are shown in the Table 1.

The channels at 0.865 and 1.24 μm are non-absorption channels present on MODIS for remote sensing of vegetation and clouds (atmospheric window channels). The channels at 0.936, 0.940, and 0.905 μm are water vapor absorption channels with decreasing absorption coefficients. The strong absorption channel at 0.935 μm is most useful for dry conditions, while the weak absorption channel at 0.905 μm is most useful for very humid conditions, or low solar elevation. The algorithms are adopted to retrieve PWV on a 2-channel ratio of an absorption channel with a window channel and a 3-channel ratio of an absorption channel with a combination of two window channels. Gao has elaborated on the details of the algorithms (Gao and Kaufman, 1998, 2003). Seeman compared the MODIS-derived PWV and radiosonde based PWV data, and concluded that MODIS PWV data was described with mean accuracy within 4.12 mm (Seemann et al., 2003).
PWV values were calibrated with Equation (1):

$$PWV = scale \times DN + offset \tag{1}$$

Where PWV is precipitable water vapor (cm), DN is the value in the original PWV layers, $scale$ and $offset$ are respectively valued as 0.001 and 0. After calibration, all data were re-projected and composed for the whole study region. The pixels of intersection region were processed with the method of maximum value composite.

Ground-based SVP data

Ground-based SVP data were calculated based on observations of 37 meteorological stations in Haihe River Basin (Figure 1). The original daily meteorological dataset was provided by China meteorological data sharing service system (CMDSSS) of China meteorological administration (CMA). Daily mean surface temperature and daily mean relative humidity were utilized to calculate SVP. Firstly, the saturation vapor pressure was calculated with following Equation:

$$e_s = 0.6107 e^{(\frac{17.38T}{239.0+T})} \tag{2}$$

Where e_s is the saturation vapor pressure (kPa), and T is the surface temperature (℃) (Abbott and Tabony, 1985). And then the saturation vapor pressure and relative humidity were used to calculate the SVP with Equation 3:

$$e = e_s \times RH \tag{3}$$

Where e is the SVP (kPa), and *RH* is relative humidity (%). Daily mean SVP dataset were generated from January, 2005 to April, 2009. SVP data from 2005 to 2008 were used for correlation analysis and model establishment, whereas the SVP data for 2009 were adopted for results validation.

Methods

Correlation analysis between MODIS-derived PWV and in-situ SVP

PWV dataset from MOD07_L2 products consists of three layers, that is the total column precipitable water vapor (PWV_T), precipitable water vapor at low level (PWV_L) and precipitable water vapor at high level (PWV_H). The correlation analysis was carried out between *in-situ* SVP and three types of PWV data respectively to determine the most suitable one for SVP estimation. At each station, daily mean SVP and PWV data of corresponding pixels from January, 2005 to December, 2008 were used for regression analysis. The correlation coefficients varied from site to site.The results were listed in detail in Table 2.

It is shown in Table 2 that PWV_L has the closest relationship with SVP in Haihe River Basin. The correlation coefficients between PWV_L and SVP are highest in the three PWV layers, whose average correlation coefficient has reached 0.911 with the maximum of 0.939 and minimum of 0.899. According to the analysis above, it can be concluded that MODIS-derived PWV_L is more suitable to model SVP than PWV_H and PWV_T. Meanwhile, the spatial diversity of correlation between PWV and SVP is relatively small (Table 3). It indicates that a valuable statistical model may be established for SVP estimation. Then we established regression models using three kinds of PWV, the details of models are shown in Table 3. It is found that the models with variable PWV_L are better than with PWV_T and PWV_H, which shows consistent result with that of correlation analysis.

Time-series analysis of the relation between MODIS-derived PWV and in-situ SVP

Karalis studied the relationship between precipitable water and surface moisture parameters in Athens and reported that their

Table 2. Correlation coefficients between daily MODIS-derived PWV and daily *in-situ* SVP from January, 2005 to December, 2008. Maximal, minimal and average values of correlation coefficients at 37 meteorological stations in Haihe River Basin were calculated.

	Maximum	Minimum	Average
PWV_H	0.902	0.823	0.862
PWV_L	0.939	0.899	0.911
PWV_T	0.926	0.887	0.907

relationship varied with season and month (Karalis, 1974). Dominated by semi-humid continental monsoon climate, it was wet in summer with plenty of precipitation and dry in winter at Haihe River Basin. A time-series analysis was conducted to investigate the seasonal variation of relationship between MODIS-derived PWV and *in-situ* SVP. Monthly averaged SVP data of all 37 meteorological stations and corresponding MODIS-derived PWV (PWV_L, PWV_T, PWV_H) data were adopted for regression analysis. The monthly variation of the correlation coefficients is shown in Figure 2.

The correlation coefficients between PWV_H and SVP varied from 0.15 to 0.6, with an average of 0.41. The profile of correlation coefficients between PWV_T and SVP varied dramatically from May to September. As shown in Figure 2, the black dash line reflects the two valley values (0.11) in June and August as rainy seasons in Haihe River Basin with most precipitation and highest air temperature of a year. As explained by Karalis that the correlation coefficients between PWV and SVP were generally quite low during the warm period of the year (Karalis, 1974). Karalis attributed this low value of correlation coefficients in summer months to the lack of effective mechanisms resulting in vertical mixing (Karalis, 1974). Such poor relationship infers that it is not valuable to evaluate SVP from PWV_T or PWV_H. The correlation coefficients between PWV_L and SVP keep relatively stable in a year, ranging from 0.72 (January) to 0.87 (October). This investigation also indicated that MODIS-derived PWV_L is a variable closely related to SVP in Haihe River Basin and could be adopted for estimating spatial distribution of SVP in the whole region.

Establishment of SVP estimation model

The analysis of relationship between PWV and SVP in result section indicated that a SVP estimation model can be established with MOD07 PWV_L in Haihe River Basin. Several kinds of models related to SVP and PWV were tested, such as simple multiples models, logarithmic models, linear models and quadratic curve (Monteith, 1961; Idso, 1969; Reber and Swope, 1972; Yang and Xue, 1996; Li et al., 2009). However, the models were different from each other in the coefficients of variable and accuracy of results, which might due to different training data and different regions adopted among these models. A suitable model is necessarily needed to evaluate SVP from MOD07 PWV_L in Haihe River Basin. The results of liner model, quadratic polynomial model and cubic polynomial model were compared, as shown in Table 4.

The regression R^2 of three models are high with the liner model of 0.831, quadratic polynomial model of 0.871 and cubic polynomial model of 0.871. With comparisons on the SVP evaluated from PWV_L and *in-situ* measurement SVP with RMSE, the accuracy of liner model is found to be worst with RMSE of 3.178 hPa. The quadratic and cubic models are better than the liner model with RMSE 2.778 and 2.777 hPa respectively. Similar results are obtained in the index of MRE. The MRE of liner model is maximal with the value of 29.4%, whereas the MRE of quadratic and cubic ones are 11.8 and 11% respectively. The accuracies of quadratic and cubic models are quite similar, while cubic one is more complicated in calculation. Meanwhile, with considerations on the MRE of 11.8% being sufficient in the region without observation stations, the quadratic polynomial model is selected in Table 4 as the daily mean SVP estimation model in Haihe River Basin. All the training data of PWV_L versus daily mean SVP is plotted in Figure 3.

RESULTS

The data from January to April in 2009 was used to evaluate the model established in 'materials and methods'. The daily mean SVP maps were calculated with the input of MOD07 PWV_L of the quadratic polynomial model. It is shown in Figures 4a - d that the selected daily mean SVP maps of four days are evaluated according to the proposed quadratic model. The red pixels reflect regions with no data, where data of the original MOD07 PWV_L are missing or with poor quality. It is shown in Figure 5 that a good spatial variation of daily mean SVP exists in Haihe River Basin.

Four examples of SVP map have the same trends of spatial distribution with the SVP increasing from west to east. It is similar to the trends of elevation in Haihe River Basin (Figure 1), which coincides the conclusion of Jolly that there are some relationships but not close between elevation and SVP (Jolly et al., 2005). Meanwhile, a slighter increase exists in the value of four maps with the time, which can be caused by the monsoon climate condition of Haihe River Basin mentioned before.

To study the accuracy of model more exactly, a comparison is conducted between the evaluation value and *in-situ* measurement value. The ground-based measured daily mean SVP of 37 stations is calculated according to the Equation 2 and 3. The contaminated pixels as red ones of no data in Figure 4 are abandoned.

With comparisons on daily mean SVP from January to April, 2009 estimated by the proposed algorithm, the calculated results from ground-based measurements generate a MRE of 17.6% higher than that of 11.8% while the SVP modeling with training data. Their slope and R^2 of a y=x line analysis were 0.918 and 0.838 respectively (Figure 5).

It is shown in Figure 5 that the difference is slight between estimated value with the model and ground-based measurements of daily SVP in Haihe River Basin. With considerations on the error brought from *in-situ* measurement and advantage of temporal and spatial result continuity, it is concluded that the results of the algorithm can be accepted.

Table 3. Details of the regression equations of the three kinds of PWVs.

	Variable	Model	R^2(hPa)	RMSE	MRE (%)
Liner	PWV_T	$SVP=0.568\times PWV_T+1.522$	0.822	3.259	33.8
	PWV_H	$SVP=1.399\times PWV_H+4.103$	0.623	4.744	55
	PWV_L	$SVP=2.316\times PWV_L-0.64$	0.831	3.178	29.4
Quadratic	PWV_T	$SVP= -0.0086PWV_T^2+0.973\times PWV_T -1.316$	0.868	2.808	16.1
	PWV_H	$SVP=-0.104\times PWV_H^2 +2.899\times PWV_H+1.557$	0.701	4.225	35
	PWV_L	$SVP=-0.129\times PWV_L^2+4.024\times PWV_L-4.617$	0.871	2.778	11.8

RMSE indicates root-mean-squared-error, while MRE indicates mean relative error.

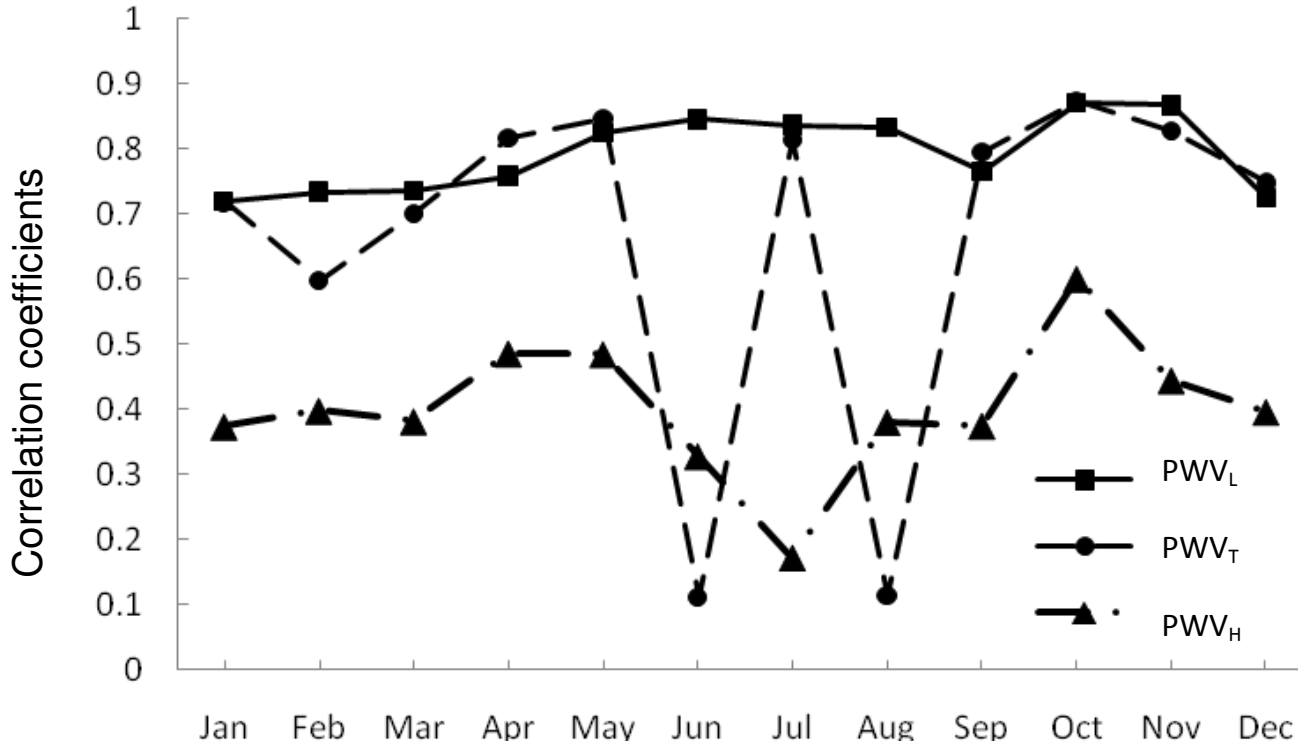

Figure 2. Monthly variation of the correlation coefficients between SVP and PWV (PWV_L, PWV_T,PWV_H) in Haihe River Basin, 2005 - 2008.

Table 4. Three types of regression models for SVP estimation from MODIS-derived PWV.

Model	Model description	R^2	RMSE (hPa)	MRE (%)
Liner	$SVP = 2.316\times PWV_L - 0.64$	0.831	3.178	29.4
Quadratic	$SVP = -0.129\times PWV_L^2 + 4.024\times PWV_L - 4.617$	0.871	2.778	11.8
Cubic	$SVP = 0.002\times PWV_L^3 - 0.17\times PWV_L^2 + 4.285\times PWV_L - 5.026$	0.871	2.777	11.0

Root-mean-squared-error, MRE: mean relative error.

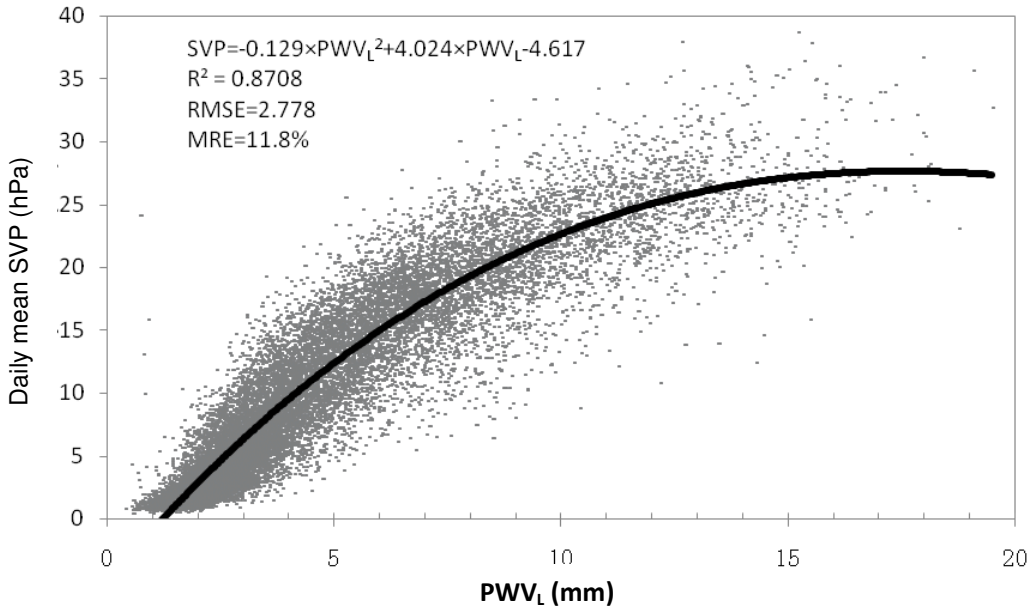

Figure 3. Scatter plot of daily mean SVP and PWV_L at 37 locations for 48 months from 2005 to 2008, in Haihe River Basin.

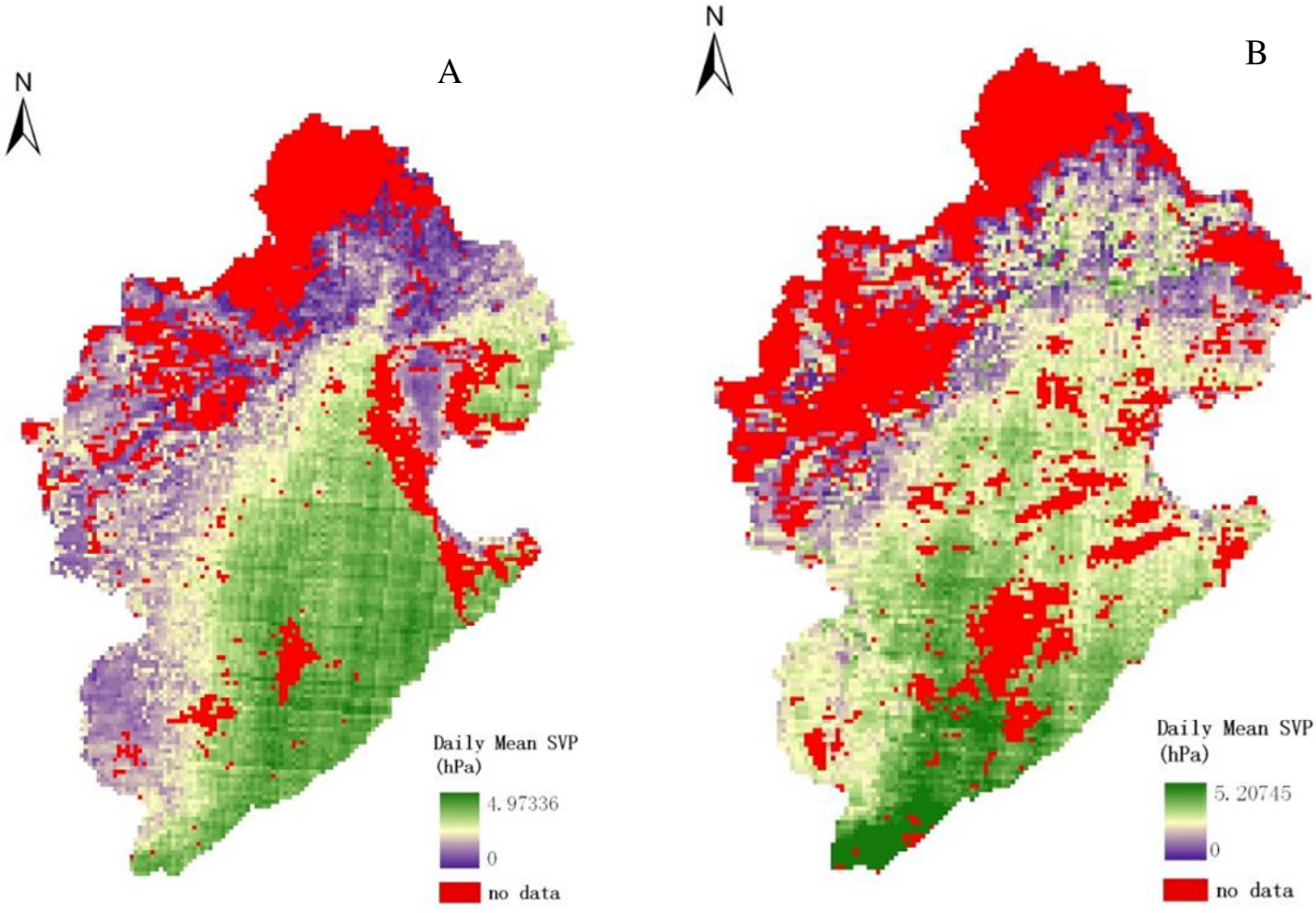

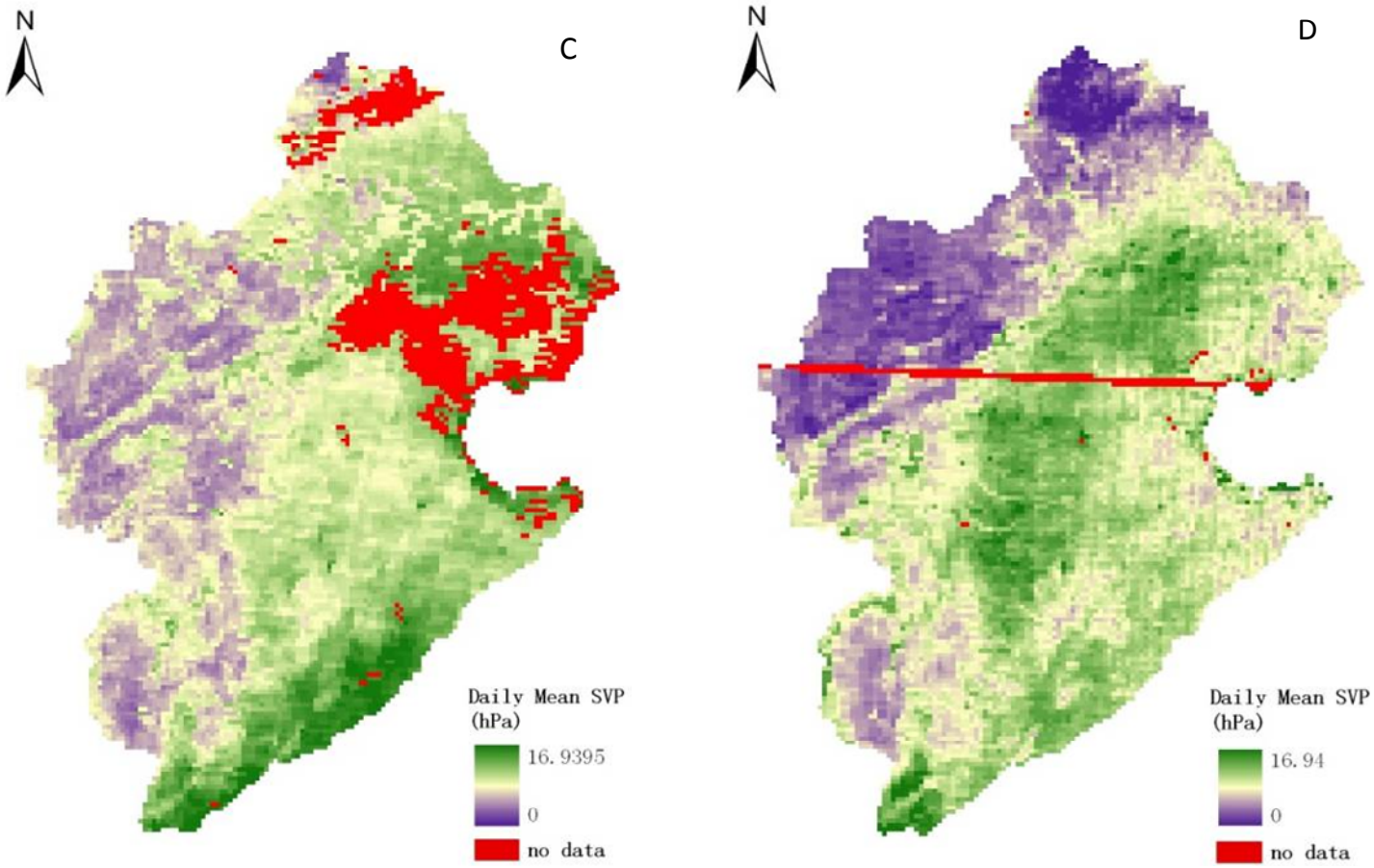

Figure 4. Daily mean SVP map estimated by the proposed model.(a) January 2, 2009 (b) February 3(c) March 18, 2009 (d) April 9, 2009.

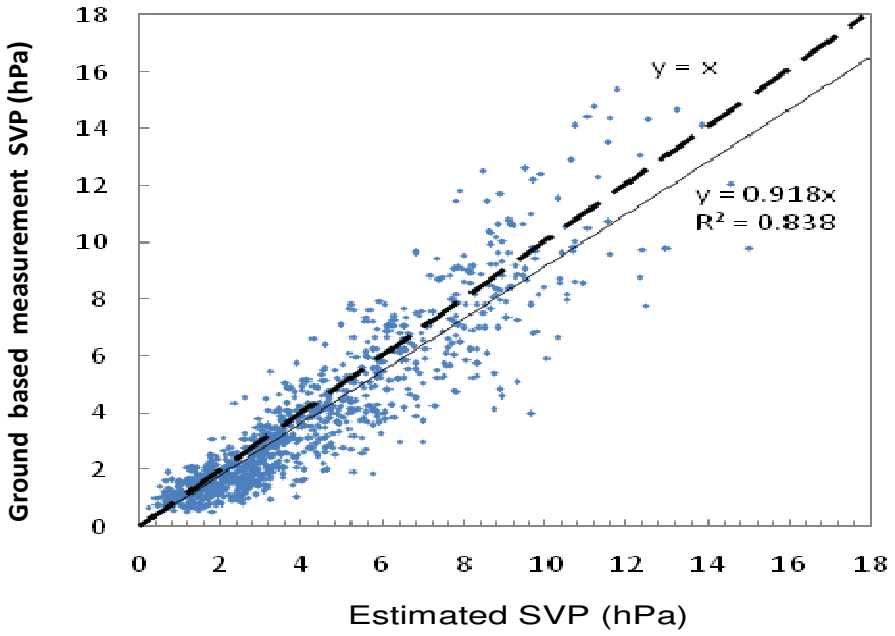

Figure 5. Scatter diagram of daily mean SVP of estimated by PWV-SVP model versus that by ground-based in Haihe River Basin during January to April, 2009.

DISCUSSION

Daily MOD07_L2 product provides PWV with a resolution of 5 km, which is strongly related to daily mean SVP. The correlation analysis was conducted between three layers of satellite-derived PWV and daily mean SVP calculated from ground-based measurement, showing that PWV had a more excellent relationship with SVP. The relatively stable correlation coefficients can be used for estimating daily mean SVP in Haihe River Basin routinely. According to the results of the correlation analysis, a quadratic polynomial model was selected for estimating daily mean SVP map in Haihe River Basin. The general robustness of this approach was noted as expressed in simple quadratic curve relationships and satellite remote sensing from MODIS, which minimized the dependence on data of ground-based observations stations for evaluating daily mean SVP and provided daily spatial distribution maps of SVP. The result of validation by testing data shows that the proposed model has acceptable precision with MRE of 17.6%.

Several points are deemed as resulting in the error of the result of SVP estimation, including the error brought from scaling-down the satellite-derived PWV raster data to point data, the error of daily mean SVP of ground-based measurement calculated by Equations 2 and 3, and the error of original data sources of satellite data. These problems are to be improved in further researches.

ACKNOWLEDGEMENTS

This work was supported by the Ministry of Science and Technology of China (Grant No. 2006CB403400-5) and the Ministry of Environmental Protection of China (Grant No. 2008BAC34B06). The authors would also like to thank the anonymous reviewers for their helpful comments and suggestions.

REFERENCES

Abbott PF, Tabony RC (1985). The estimation of humidity parameters. Meteorol. Mag., 114: 49-56.

Barton IJ, Prata AJ (1999). Difficulties associated with the application of covariance-variance techniques to retrieval of atmospheric water vapor from satellite imagery. Rem. Sens. Environ., 69: 76-83.

Bevis M, Businger S, Herring TA, Anthes RA, Rocken C, Ware RH, Chiswell SR (1994). GPS Meteorology: Mapping zenith wet delays onto precipitable water vapour. J. Appl. Meteorol., 33: 379-386.

Brooker P (1979). Kriging. Engr. Min. J., 180: 148-153.

Chylek P, Borel CC (2003). Columnar water vapor retrieval using multispectral satellite data. Recent Research Developments in Atmospheric Sciences. LA-UR-03-1414 (Available at: http://cborel.net/CWV03.pdf).

Duan J, Bevis M, Fang P, Bock Y (1996). GPS Meteorology: Direct estimation of the absolute value of precipitable water vapour. J. Appl. Meteorol., 35(6): 830-838.

Gao BC, Kaufman YJ (1998). The MODIS near-IR water vapor algorithm. Product ID: MOD05 – Total precipitable water. Algorithm Technical Background Document ATBD-MOD-03 (Available at: http://modis.gsfc.nasa.gov/data/atbd/atbd_mod03.pdf).

Gao BC, Kaufman YJ (2003). Water vapor retrievals using Moderate Resolution Imaging Spectroradiometer (MODIS) near-infrared channels. J. Geophys. Res., 108: 4389.

Green RM, Hay SI (2002). The potential of Pathfinder AVHRR data for providing surrogate climatic variables across Africa and Europe for epidemiological applications. Rem. Sens. Env. 79:166-175.

Hashimoto H, Dungan JL, White MA, Yang FH (2008). Satellite-based estimation of surface vapor pressure deficits using MODIS land surface temperature data. Rem. Sens. Environ., 112: 142-155.

Hong G, Yang P, Baum AB, Heymsfield AJ (2008). Relationship between ice water content and equivalent radar reflectivity for clouds consisting of nonspherical ice particles. J. Geophys. Res., 113(D20), D20205.

http://modis.gsfc.nasa.gov/index.php

http://modis-atmos.gsfc.nasa.gov/MOD07_L2/index.html

http://www.ae.utexas.edu/courses/ase389p_gps/projects99/whitlock/intro.html

Hutchinson MF, Gessler PE (1994). Splines-More than just a smooth interpolator. Geoderma, 62: 45-67.

Idso BS (1969). Atmospheric attenuation of solar radiation. J. Atmos. Sci., 26: 1088-1095.

Jolly WM, Graham JM, Michaelis A, Nemani RR, Running SW (2005). A flexible, integrated system for generating meteorological surfaces derived from point sources across multiple geographic scales. Environ. Model. Software, 20: 873-882.

Karalis JD (1974). Precipitable Water and It s Relationship to Surface Dew Point and Vapor Pressure in Athens. J. Appl. Meteorol., 13(1): 760-766.

Kern A, Bartholy J, Borbas EE, Barcza Z, Pongracz R, Ferencz C (2008). Estimation of vertically integrated water vapor in Hungary using MODIS imagery. Adv. Space Res., 41: 1933-1945.

Li GC, Li GP, Liu FH, Miao ZC (2009). Characteristics of Precipitable Water Vapor and Their Relation-Ship with Surface Vapor Pressure in North China. J. Trop. Meteorol., 25(4): 488-494.

Monteith JL (1961) An empirical method for estimating long-wave radiation exchanges in the British Isles. Q. J. Roy. Meteorol. Soc., 87: 171-179.

New M, Hulme M, Jones P (1999). Representing twentieth-century space–time climate variability. Part I: Development of a 1961–90 mean monthly terrestrial climatology. J. Climate, 12: 829-856.

Ottle C, Outalha S, Francois C, Le MS (1999a). Estimation of atmospheric water vapor content from split-window radiance measurements. Rem. Sens. Environ., 61: 410-418.

Ottle C, Francois C (1999b). Further insights into the use of the split-window covariance technique for precipitable water retrieval. Rem. Sens. Environ., 69: 84-86.

Prince SD, Goetz SJ, Dubayah RO, Czajkowski KP, Thawley M (1998). Inference of surface and air temperature, atmospheric preipitable water and vapor pressure deficit using Advanced Very High-Resolution Radiometer satellite observations:comparison with field observations. J. Hydrol., pp. 212-213, 230-249,

Reber EE, Swope JR (1972). On the Correlation of the Total Precipitable Water in a Vertical Column and Absolute Humidity at the Surface. J. Appl. Meteorol., 11(2): 1322-1325.

Seemann SW, Li J, Menzel WP (2003). Operational Retrieval of Atmospheric Temperature, Moisture, and Ozone from MODIS Infrared Radiances. J. Appl. Met., 42(8): 1072-1091.

Thiessen AH (1911). Precipitation averages for large areas. Mon. Weather. Rev., 39: 1082-1084

Thornton PE, Running SW, White MA (1997). Generating surfaces of daily meteorological variables over large regions of complex terrain. J. Hydrol., 190: 214-251.

Waring RH, Running SW (1998). Forest ecosystems: Analysis at multiple scales. San Diego: Academic Press.

Watson DF, Philip GM (1985). A refinement of inverse distance weighted interpolation. Geo. Process, 2: 315-327.

Westwater ER, Han Y, Shupe MD, Matrosov SY (2001). Analysis of integrated cloud liquid and precipitable water vapor retrievals from microwave radiometers during the surface heat budget of the Arctic Ocean project. J. Geophys. Res. 106(D23): 32019-32030.

Yang JM, Xue JH (1996). The empirical expressions of the relation between precipitable water and ground water vapor pressure for some areas in China. Chin. J. Atmos. Sci., 20(5): 620-626.